SUPPLEMENTARY INFORMATION

Reversibly Trapping Visible Laser Light through the Catalytic Photo-oxidation of I^- by $Ru(bpy)_3^{2+}$

Derek. R. Morim, Ignacio Vargas-Baca*, Kalaichelvi Saravanamuttu*

Department of Chemistry and Chemical Biology, McMaster University,
1280 Main Street West, Hamilton, Ontario, L8S 4M1, Canada
email : kalai@mcmaster.ca
email: vargas@chemistry.mcmaster.ca

*Corresponding Authors

Kalaichelvi Saravanamuttu
Associate Professor
Phone: 9055259140 ext. 24615
email : kalai@mcmaster.ca

Ignacio Vargas-Baca
Associate Professor
Phone: 9055259140 ext. 23497
email: vargasi@ mcmaster.ca

Department of Chemistry and Chemical Biology
McMaster University
1280 Main Street West
Hamilton, Ontario L8S4M1
Canada

Table of Contents

Section S1. Experimental Methods
S1a. Materials……..S3
S1b. Preparation of Pluronic F-127 gels for optical self-trapping……..…..S3
S1c. Optical assembly…….....S3
S1d. Instrumental techniques……...S5
S1e. Control experiments……S5
S1f. Quenching studies with methyl viologen……..S5
Section S2. Intensity dependence of optical self-trapping……....S7
Section S3. Optical self-trapping due to a secondary photo-oxidative process……..…S12
Section S4. Description of movies……..S32
Section S5. References……..……...……....S32

Section S1. Experimental Methods

S1a. Materials

Methyl orange (Fisher Scientific Co.), fluorescein sodium salt (Aldrich), rhodamine B (Aldrich), methyl violet (Aldrich), tris(bipyridine)ruthenium(II) chloride hexahydrate (Strem Chemicals Inc.), Pluronic® F-127 polymer (Sigma-Aldrich), methyl viologen dichloride hydrate (Aldrich), and tetramethylorthosilicate (Aldrich) used without further purification. Furfuryl alcohol (Aldrich) was distilled under reduced pressure.

S1b. Preparation of Pluronic® F-127 gels for optical self-trapping

Gels were made by preparing a 25 wt. by wt.% solution of Pluronic® F-127 polymer below its lower critical solution temperature (LCST) by dissolving the polymer with a glass rod in deionized H_2O (Milli-Q®, 18.2 MΩcm) surrounded by an ice bath. Equilibration to room temperature results in the formation of a gel due to the dehydration of the PPO segments of the triblock copolymer.

Doped gels were prepared by substituting deionized water with an aqueous solution of the desired dopant(s) in deionized water. Different concentrations were utilized, but optimal self-trapping was achieved for 1.3 mM $Ru(bpy)_3Cl_2$ and 0.2 M NaI. Samples without iodide contained 80 μM tris(bipyridine)ruthenium(II) chloride hexahydrate.

Samples for optical experiments were prepared by transferring the solutions below their LCST into cylindrical cells (diameter = 12 mm, pathlength = 6 mm) with optically flat, transparent windows.

S1c. Optical assembly

Self-trapping experiments were carried out on an optical assembly adapted from previous studies.[1] The excitation source was the TEM_{00} mode (Gaussian beam, M2 < 1.1) of c,w. visible (532 nm) light emitted by a diode-pumped solid-state laser (Verdi V2, Coherent, Inc., California, USA). The output beam, which had a diameter 2.25 mm and power of 500 mW, was passed through a $\lambda/2$ waveplate, polarizing beam splitter cube and neutral density filter. The $\lambda/2$ waveplate orientation was adjusted to obtain the required intensity and the attenuated beam was guided by a pair of 45° elliptical mirrors onto a planoconvex lens [focal length = 75.6 mm], which focused the beam to a diameter of 20 μm onto the entrance window of the sample cell containing the sample.

The spatial intensity profile of the beam at the exit face of the cell was imaged by a pair of planoconvex lenses (f. l. = 75.6 mm and f. l. = 300.0 mm) onto a high-resolution charge-coupled device (CCD) camera [736 horizontal× 484 vertical pixels; pixel size = 4.80 μm horizontal × 5.58 μm vertical; LaserCam IIID 1⁄400, Coherent, Inc., California, USA]. Combinations of neutral density filters (F) mounted on three separate rotatable wheels (VARM, Coherent, Inc.) were placed between

imaging lenses to prevent saturation of the CCD camera. All imaging optical components could be translated along the *z* direction with a resolution of 0.25 mm. Images were collected every second for the first 256 s and then every 20 s afterwards. The camera used BeamView Analyzer software (Version 3.2), which calculates beam diameter ($1/e^2$) and relative peak intensity, generates two-dimensional (2D) and three-dimensional (3D) intensity profiles and corrects for image magnification by the lenses (×4.0). The effective beam diameter corresponds to the circular area of all pixels with relative intensity > 13.5% ($1/e^2$) of the maximum (peak) intensity. The relative peak intensity is the ratio between the greatest intensity on one or more pixels in an image and the saturation intensity of the camera.

Intensities ranging from 6.4 Wcm^{-2} to 318.0 Wcm^{-2} were employed for experiments of self-trapping. For experiments probing the reversibility of self-trapping in samples without NaI, the laser beam was blocked after self-trapping had begun and then unblocked after a specific amount of time had lapsed. For samples containing NaI, the beam intensity was decreased by 100-fold in order to passively monitor the beam size.

Plots of spatially intensity profiles of the beam were generated with the SigmaPlot™ software.

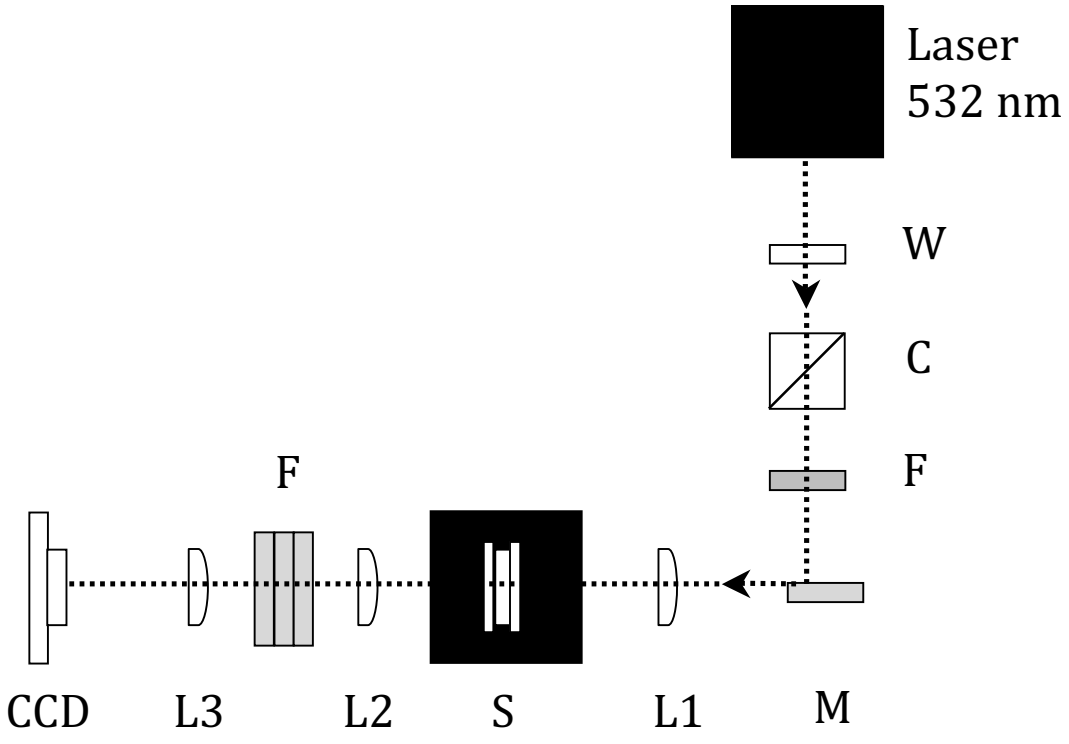

Figure S1 Optical assembly for self-trapping.[1]

S1d. Instrumental techniques

UV-Visible spectroscopy

Absorbance spectra were acquired by a Cary 50 spectrophotometer (Agilent Technologies). Fluorescence measurements were carried out on a Cary 50 Eclipse spectrophotometer (Agilent Technologies).

An aqueous solution and separately, a Pluronic® F-127 gel of tris(bipyridine)ruthenium(II) chloride with and without NaI was irradiated in a quartz cuvette for 10 hrs. with a 532 nm (20 mW) beam. Absorbance spectra were acquired before and after irradiation to identify photoproducts and photodecomposition. Fluorescence spectroscopy was used for the Stern-Volmer study.(Section S1f.).

Differential scanning calorimetry was carried out on a Q20 Differential Scanning Calorimeter (TA Instruments). Measurements were made of the 25 wt. by wt. % Pluronic® F-127 gels with and without $Ru(bpy)_3Cl_2$; scans of each sample were acquired before and after irradiation (3 hrs., 532 nm, 40 $mWcm^{-2}$). Samples were prepared and weighed in tzero hermetic sample cells; an empty tzero hermetic sample cell served as the reference. A heating/cooling rate of 0.2 $°Cmin^{-1}$. was employed.

S1e. Control experiments

Pluronic® F-127 gels were prepared from solutions of tris(bipyridine)ruthenium (II) chloride (80 μM). A sample was made with a solution of 100 mM of methyl orange to determine if optical self-trapping originates through a thermal mechanism.

Pluronic® F-127 gels doped with different luminescent chromophores, fluorescein sodium salt (400 μM), rhodamine B (400 μM), and methyl violet (5 mM), were prepared to probe whether luminescence and excitation to a triplet state is a requirement for self-trapping.

To determine the effect of singlet oxygen scavengers on the rate of self-trapping, furfuryl alcohol (0.17 M) was added to a gel containing 80 μM $Ru(bpy)_3Cl_2$.

To probe the role of the Pluronic® F-127 gel matrix on self-trapping, samples were also prepared from a siloxane glass (0.54 M tetramethylorthosilicate; 12 μM $Ru(bpy)_3Cl_2$ in water).

S1f. Quenching studies with methyl viologen

Aqueous solutions of tris(bipyridine)ruthenium(II) chloride (80 μM) and methyl viologen dichloride hydrate with concentrations ranging from 0 mM-12 mM were prepared and degassed with water-saturated Ar immediately prior to acquiring their fluorescence spectra. Stern-Volmer plots were prepared by plotting relative

fluorescence intensity against the concentration of methyl viologen quencher; the Stern-Volmer constant was obtained according to:

$$\frac{I^0{}_f}{I_f} = 1 + k_q \tau_0 \bullet [Q] \qquad \text{[S1]}$$

The above-mentioned solutions were converted to Pluronic® F-127 gels for studies of optical self-trapping; absorbance and fluorescence spectra of gels were also obtained. The concentration of methyl viologen in the gel was obtained by using the absorbance spectra Because gel formation leads to a volume change, the modified concentration of methyl viologen was obtained through the absorbance spectra of the gels.

Regression analysis for Stern-Volmer plots was carried out with StatPlus, and was used to confirm that the Stern-Volmer constants obtained from self-trapping and fluorescence were statistically the same.

Section S2. Intensity dependence of optical self-trapping

Optical self-trapping with 25% Pluronic® F-127 gels containing 1.3 mM $Ru(bpy)_3Cl_2$ and 0.2 M sodium iodide was studied at intensities ranging from 3.2 Wcm^{-2} to 159 Wcm^{-2}. Figures S2-S6 summarize the temporal evolution of the beam intensity and diameter during self-trapping. Results show that the rate of self-trapping increases with incident intensity. However, at intensities > 159 Wcm^{-2}, the Gaussian beam transformed into a single ring (Figure S6); greater intensities excite large populations of I_3^- and rapidly generate a flat-top Δn profile (different from the gradient, lens-like profile required for self-trapping) across the beam. Theoretical modeling previously showed that this elicits the transformation of a Gaussian beam into a ring-like structure[2]. Upon prolonged irradiation at intensities > 6 $kWcm^{-2}$, large NaI_3 crystallites (~100 µm) accumulate and scatter light along the beam path, disrupting the self-trapping process (Figure S7). It is possible that a small amount of $Ru(bpy)_2I_2$ can also be generated at these high intensities according to Hoggard and coworkers.[3]

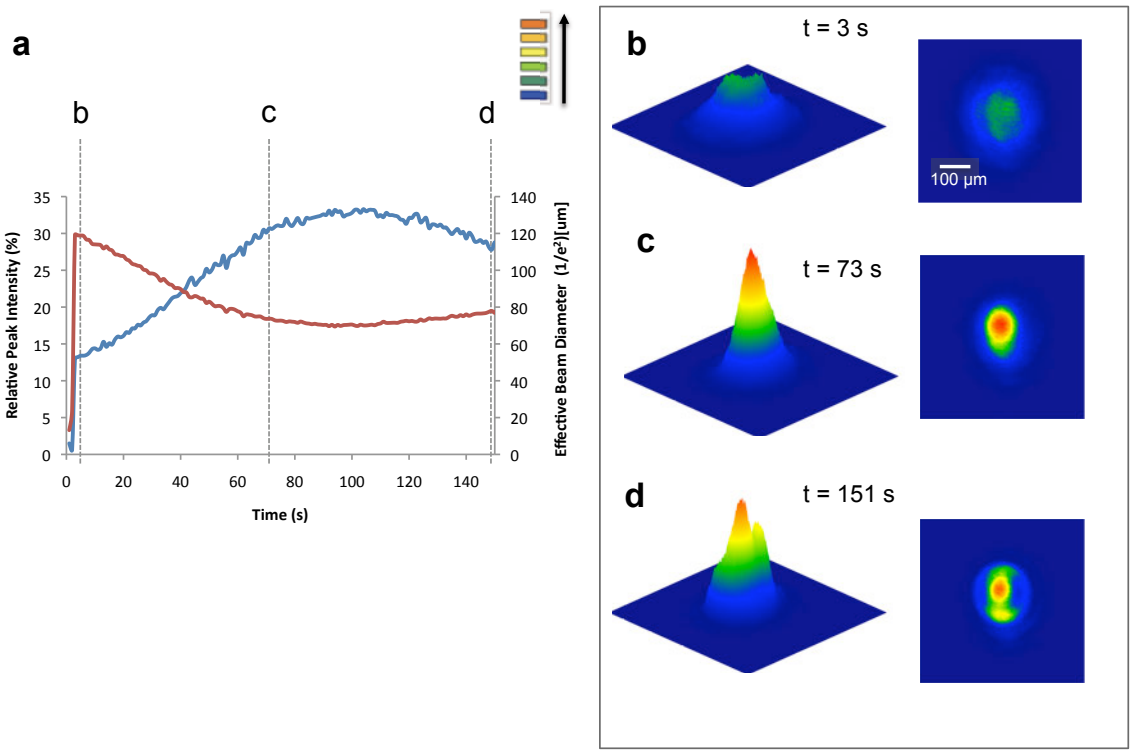

Figure S2 Optical self-trapping with Pluronic® F-127 gel containing 1.3 mM $Ru(bpy)_3Cl_2$ and 0.2 M NaI at 3.2 Wcm^{-2}. The labeled dotted lines in the (a) graph showing temporal evolution of intensity and beam width correspond to (b-d) spatial intensity profiles of the beam.

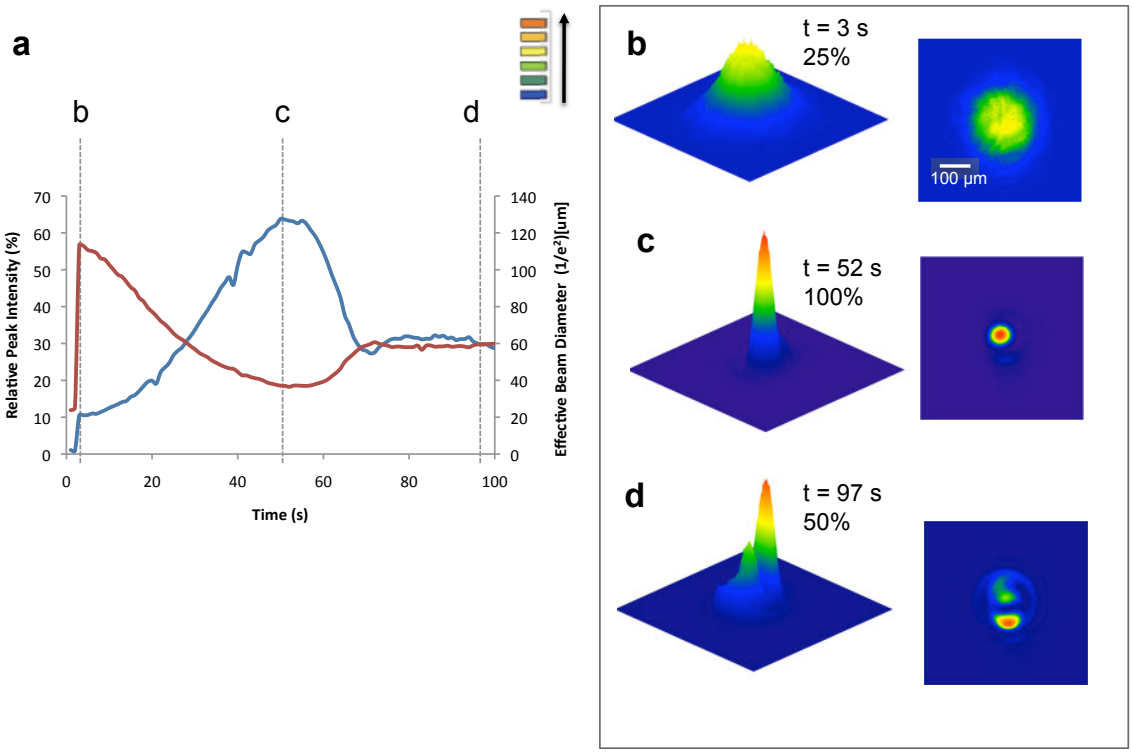

Figure S3 Optical self-trapping with Pluronic® F-127 gel containing 1.3 mM $Ru(bpy)_3Cl_2$ and 0.2 M sodium iodide at 8.0 Wcm^{-2}. The labeled dotted lines in the (a) graph showing temporal evolution of intensity and beam width correspond to (b-d) spatial intensity profiles of the beam.

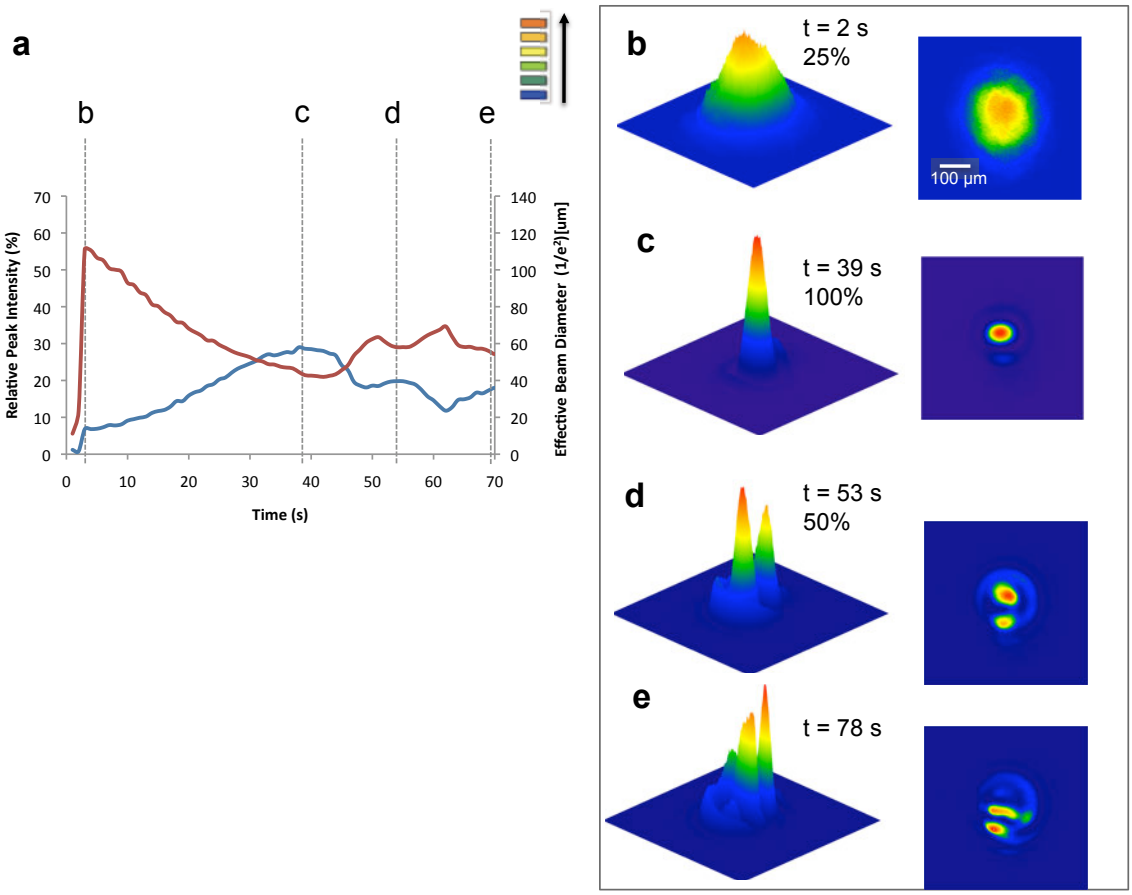

Figure S4 Optical self-trapping with Pluronic® F-127 gel containing 1.3 mM $Ru(bpy)_3Cl_2$ and 0.2 M sodium iodide at 16.0 Wcm^{-2}. The labeled dotted lines in the (a) graph showing temporal evolution of intensity and beam width correspond to (b-e) spatial intensity profiles of the beam.

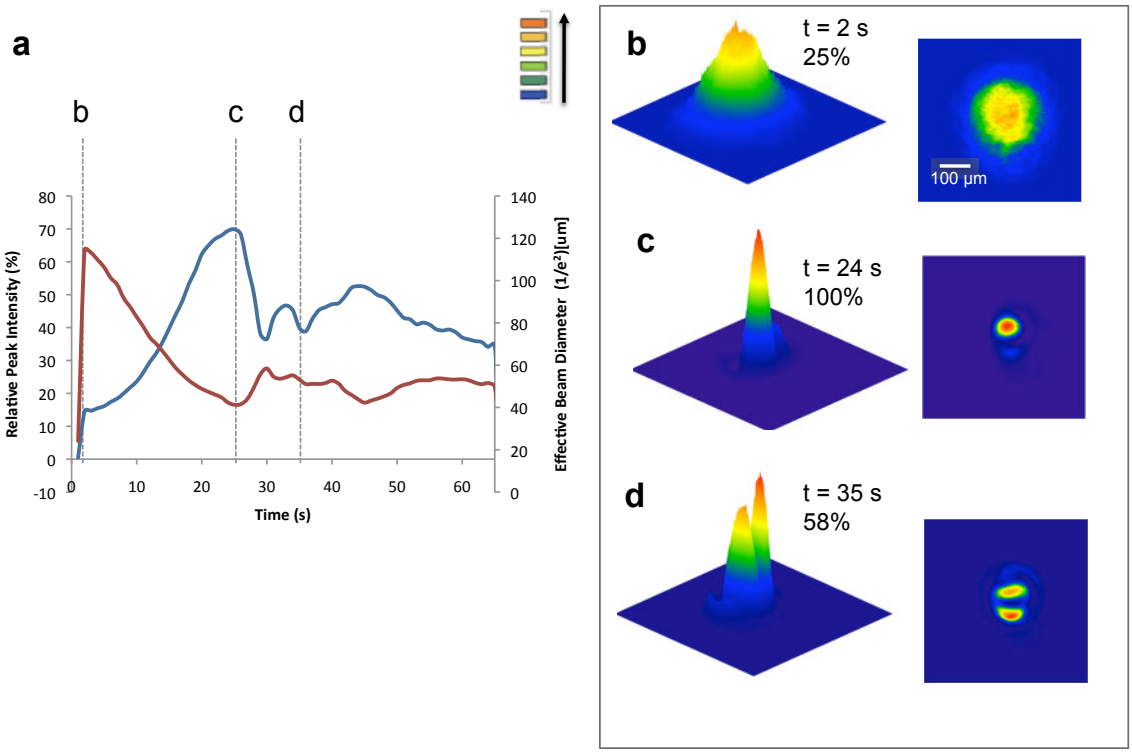

Figure S5 Optical self-trapping with Pluronic® F-127 gel containing 1.3 mM $Ru(bpy)_3Cl_2$ and 0.2 M sodium iodide at 32.0 Wcm^{-2}. The labeled dotted lines in the (a) graph showing temporal evolution of intensity and beam width correspond to (b-d) spatial intensity profiles of the beam.

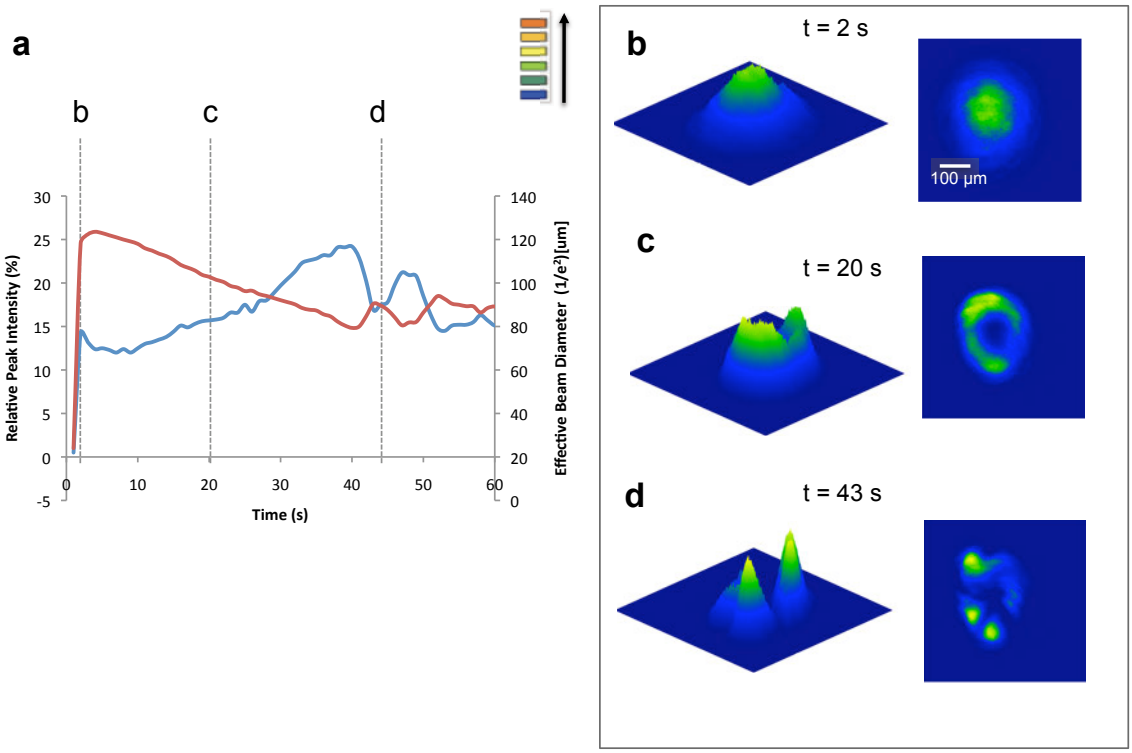

Figure S6 Optical self-trapping with Pluronic® F-127 gel containing 1.3 mM $Ru(bpy)_3Cl_2$ and 0.2 M sodium iodide at 159.0 Wcm^{-2}. The labeled dotted lines in the (a) graph showing temporal evolution of intensity and beam width correspond to (b-d) spatial intensity profiles of the beam.

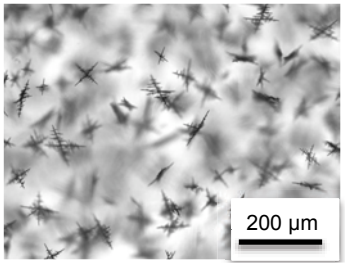

Figure S7 Optical micrograph of crystals formed after prolonged laser irradiation.

Section 3. Optical self-trapping due to a secondary photo-oxidative process

This Section describes the irreversible self-trapping that occurs in hydrogels containing $Ru(bpy)_3Cl_2$ alone in the absence of NaI. The process generates a permanent waveguide and takes over 4000 seconds to form at 159 Wcm^{-2}. The series of experiments described below suggest that Δn in this case originates from crosslinking of the Pluronic® F-127 hydrogel due to photogenerated singlet oxygen. An intensity study revealed that self-trapping is saturable, but no formation of rings occurred, most probably due to the slow evolution time within this system (Figures S8-S11).

It was confirmed that Δn in this system did not originate from laser-induced heating and phase transitions in the hydrogel[4,5,6,7]: self-trapping did not occur in hydrogels in the absence of $Ru(bpy)_3^{2+}$ (Figure S12) nor was it induced by heat dissipated by non-radiative relaxation of photoexcited chromophores; for example, self-trapping was not observed when $Ru(bpy)_3^{2+}$ was replaced with methyl orange, which has even greater absorbance at 532 nm (Figure S13).

We found that the secondary self-trapping rate decreased with increasing concentrations of quencher, methyl viologen (Figures S14-S19).[8] Stern-Volmer plots comparing the effect of methyl-viologen on secondary self-trapping rate and separately, photoluminescence of $Ru(bpy)_3^{2+}$, yielded statistically equal K_{SV} constants confirming that photoexcited $Ru(bpy)_3^{2+}$ was critical to this secondary process (Figures S20-S22). Specifically, singlet oxygen generated by $Ru(bpy)_3^{2+*}$ played a key role[9]; for e.g., there was a significant decrease in self-trapping rate in the presence of scavenger furfuryl alcohol (Figure S23).[10] The photodegradation of $Ru(bpy)_3Cl_2$ at long times is also likely due to singlet oxygen (Figure S24). Indeed, hydrogels containing a range of sensitizers capable of producing singlet oxygen including fluorescein, rhodamine b and methyl violet displayed secondary self-trapping, with the greatest rate found with chromophores possessing the largest quantum yields (Figures S25-27).[11,12]

The fluorescence intensity of $Ru(bpy)_3^{2+}$ remained unchanged by the furfuryl alcohol, indicating that the excited complex does not react directly with its gel medium (Figure S28). However, the hydrogel is essential as self-trapping was not observed in water or a siloxane matrix containing $Ru(bpy)_3^{2+}$ (Figures S29-S30). Pluronic® copolymers can enhance the production of singlet oxygen,[13] which is highly reactive towards olefins, ethers, and other electron-rich groups,[99,14,15] and can effect crosslinking of collagen gels when illuminated in the presence of a photosensitizer[16] through a complex mechanism involving several radical species including hydroxyl radicals.[17,18]

Based on the above-described observations, we conclude that singlet oxygen generated by photoexcited $Ru(bpy)_3^{2+}$ leads to the irreversible oxidation and subsequent crosslinking of the Pluronic® F-127 hydrogel (Figure S31). While matrix

densification due to cross-linking was not detected by ^{1}H NMR or IR spectroscopy, differential scanning calorimetry showed a shift of ~1ºC in the micellization temperature of the laser-irradiated Pluronic® F-127 medium containing $Ru(bpy)_3^{2+}$ (Figure S32). Crosslinking in the hydrogel localized to the beam path generates Δn, which underlies secondary self-trapping. In the presence of NaI however, the slow, secondary self-trapping is negligible and self-trapped beams can be quickly and reversibly generated.

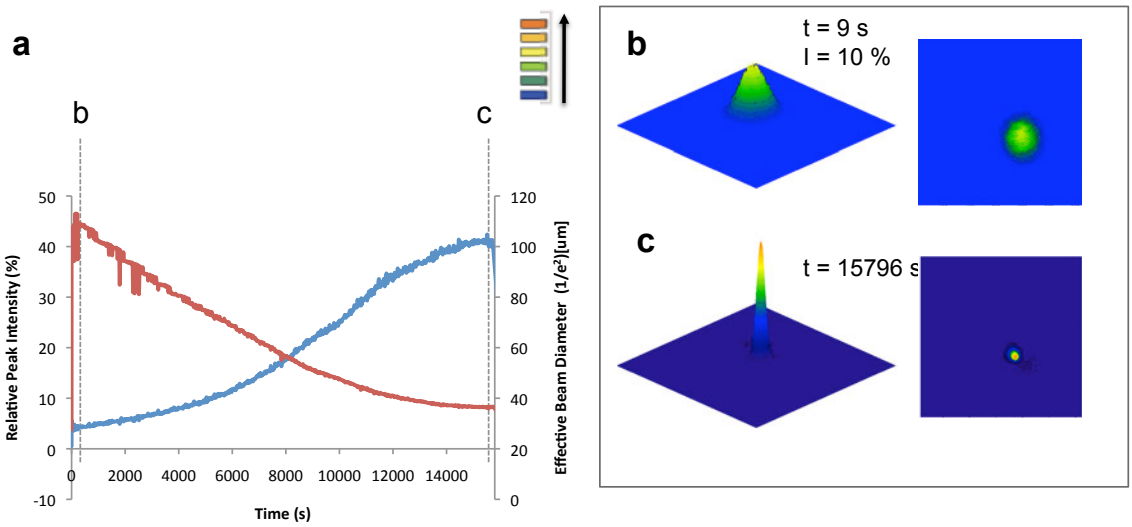

Figure S8 Optical self-trapping with Pluronic® F-127 gel containing 12 μM $Ru(bpy)_3Cl_2$ at 6.4 Wcm^{-2}. The labeled dotted lines in the (a) graph showing temporal evolution of intensity and beam width correspond to (b-c) spatial intensity profiles of the beam.

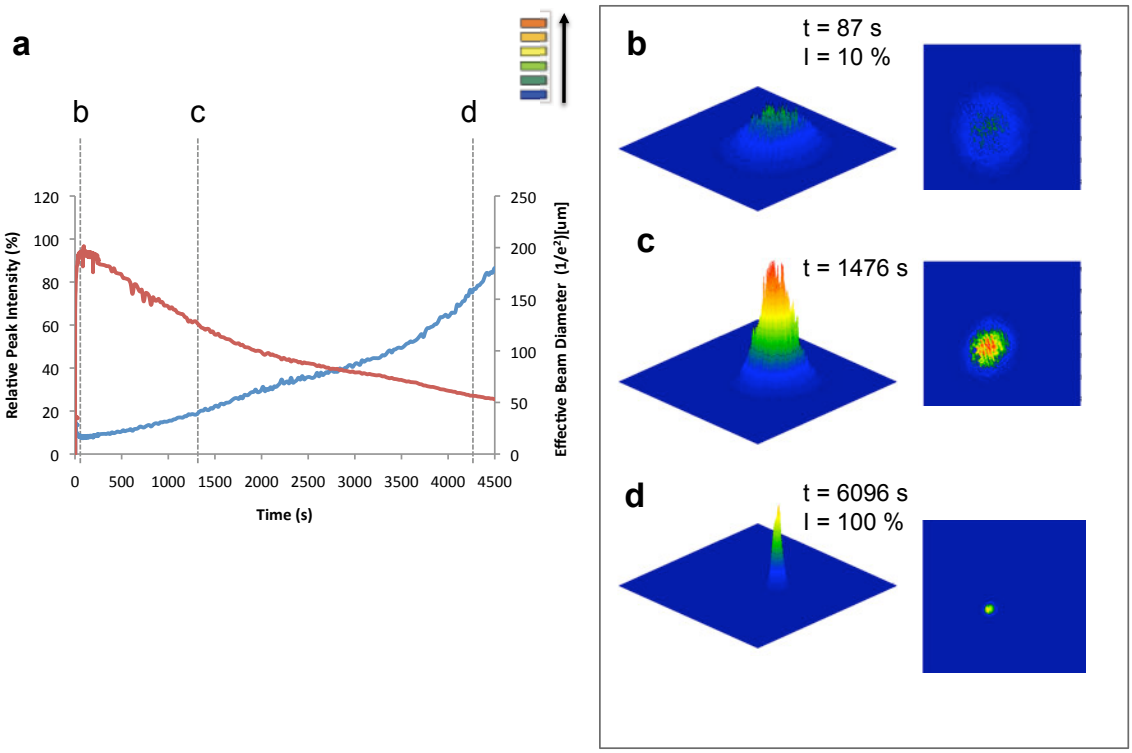

Figure S9 Optical self-trapping with Pluronic® F-127 gel containing 12 μM $Ru(bpy)_3Cl_2$ at 32 Wcm^{-2}. The labeled dotted lines in the (a) graph showing temporal evolution of intensity and beam width correspond to (b-d) spatial intensity profiles of the beam.

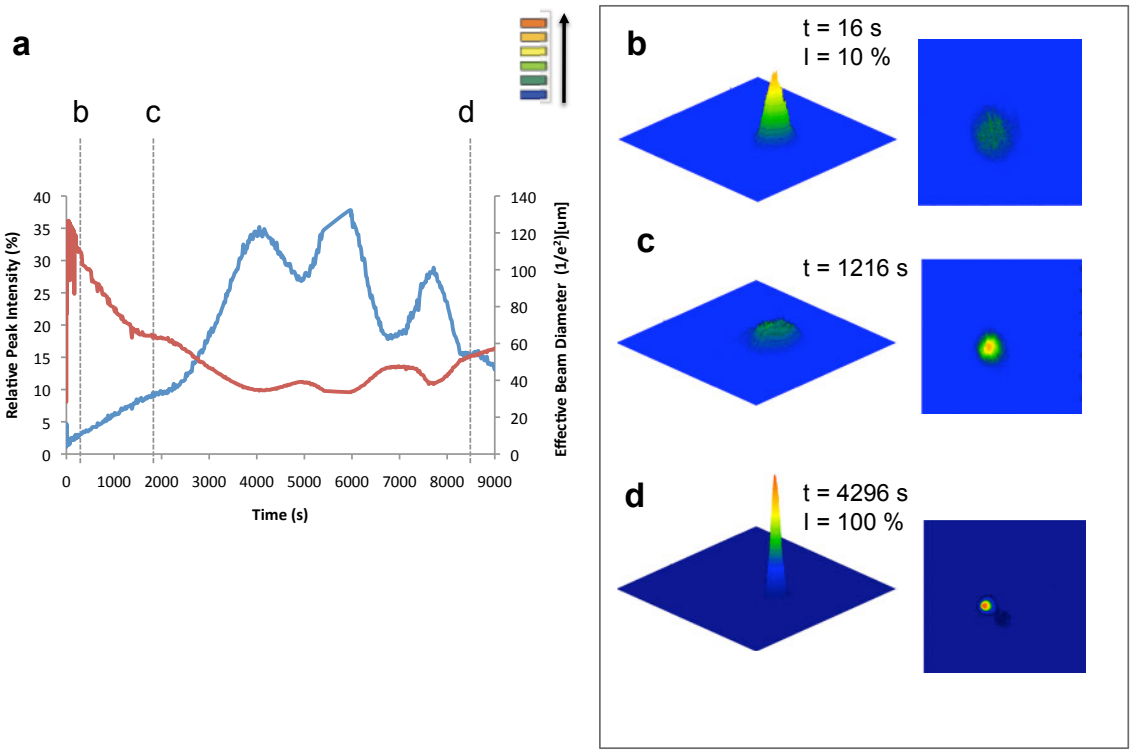

Figure S10 Optical self-trapping with Pluronic® F-127 gel containing 12 μM $Ru(bpy)_3Cl_2$ at 64 Wcm^{-2}. The labeled dotted lines in the (a) graph showing temporal evolution of intensity and beam width correspond to (b-d) spatial intensity profiles of the beam.

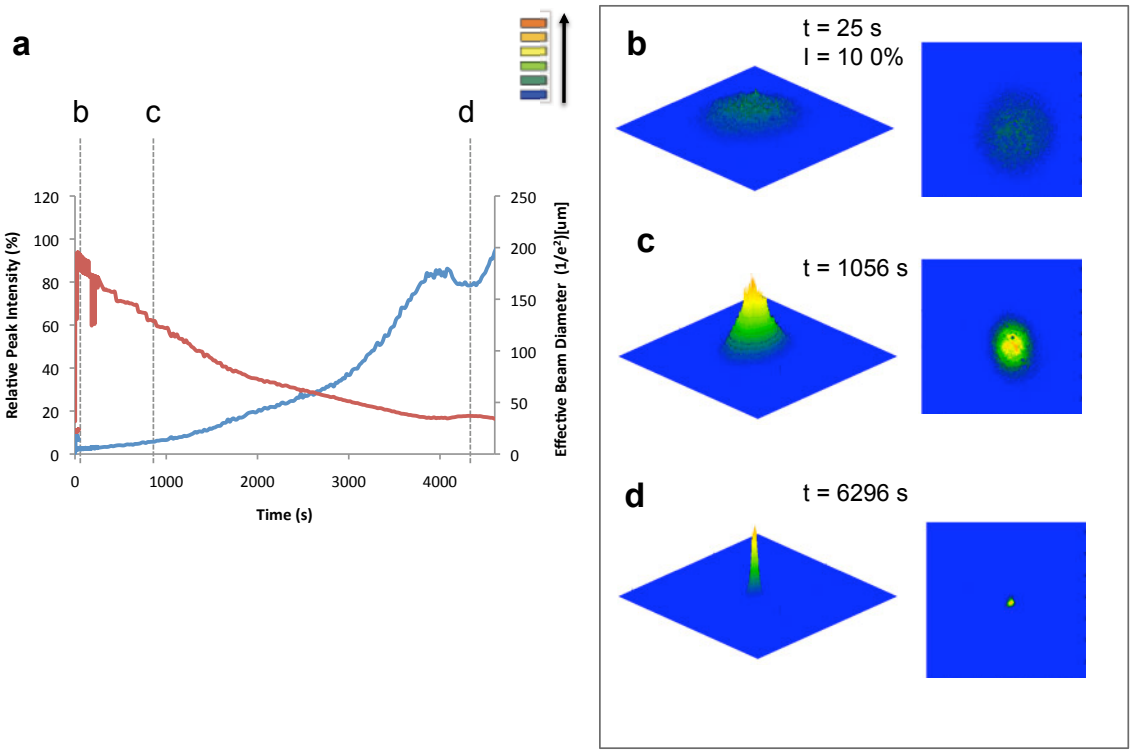

Figure S11 Optical self-trapping with Pluronic® F-127 gel containing 12 μM $Ru(bpy)_3Cl_2$ at 159 Wcm^{-2}. The labeled dotted lines in the (a) graph showing temporal evolution of intensity and beam width correspond to (b-d) spatial intensity profiles of the beam.

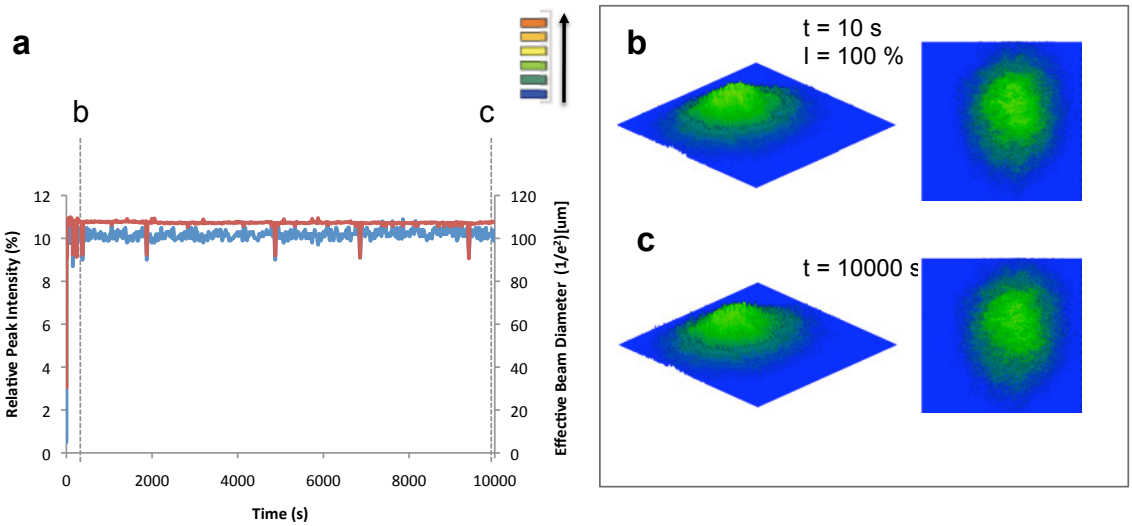

Figure S12 Optical self-trapping with Pluronic® F-127 gel at 159 Wcm^{-2}. The labeled dotted lines correspond to the included spatial intensity profiles.

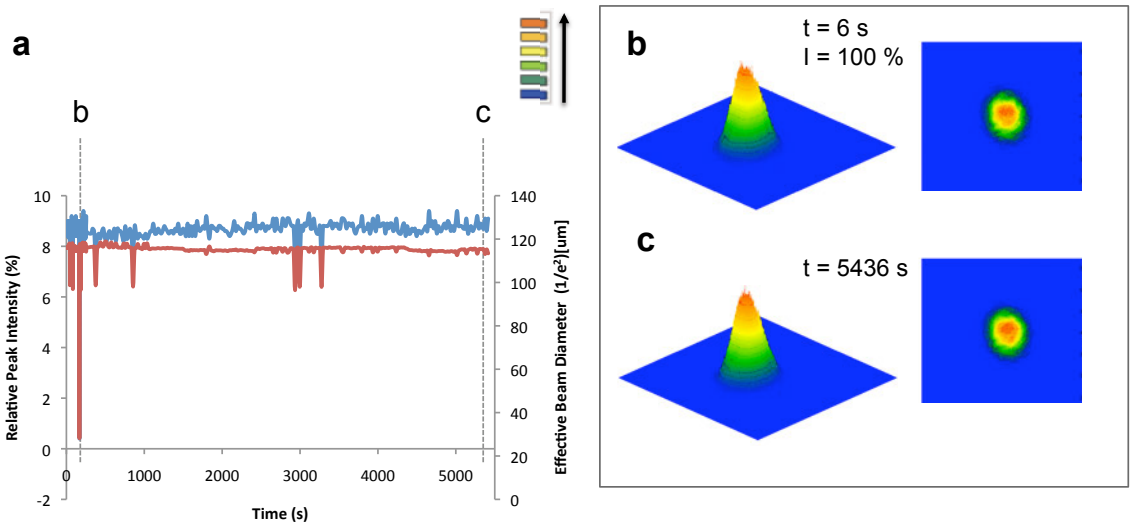

Figure S13 Optical self-trapping with Pluronic® F-127 gel containing 100 mM methyl orange at 159 Wcm^{-2}. The labeled dotted lines in the (a) graph showing temporal evolution of intensity and beam width correspond to (b-d) spatial intensity profiles of the beam.

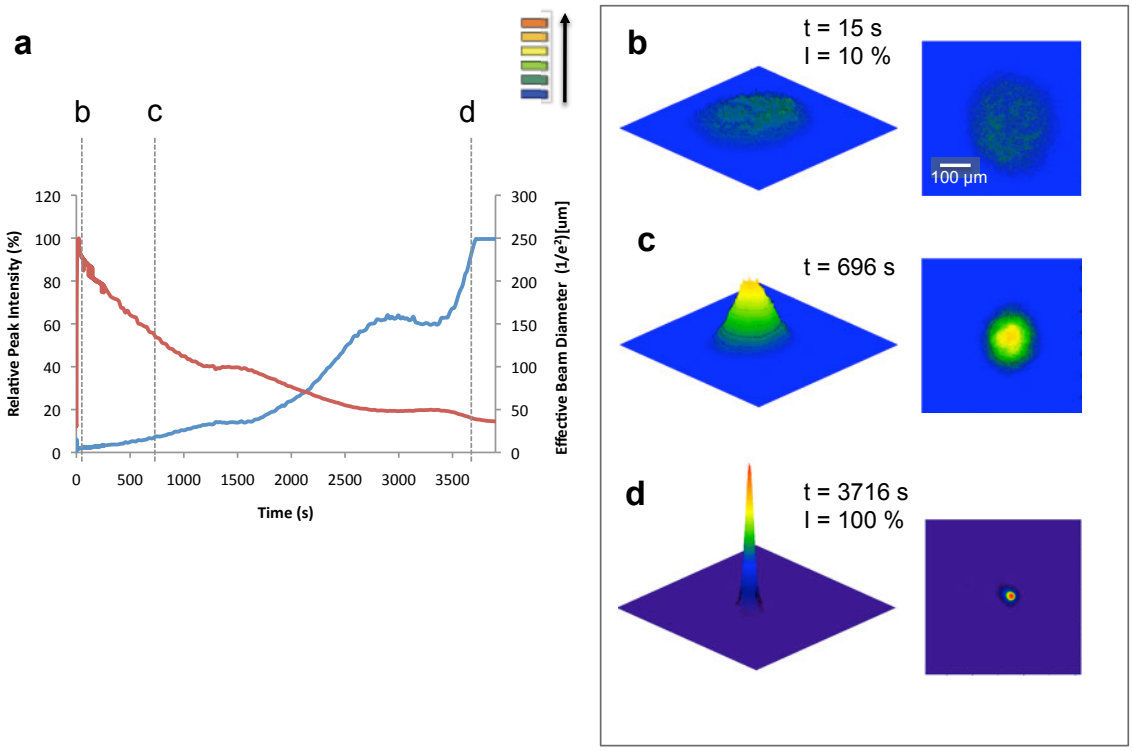

Figure S14 Optical self-trapping with Pluronic® F-127 gel containing 80 µM $Ru(bpy)_3Cl_2$ and no methyl viologen at 159 Wcm^{-2}. The labeled dotted lines in the (a) graph showing temporal evolution of intensity and beam width correspond to (b-d) spatial intensity profiles of the beam.

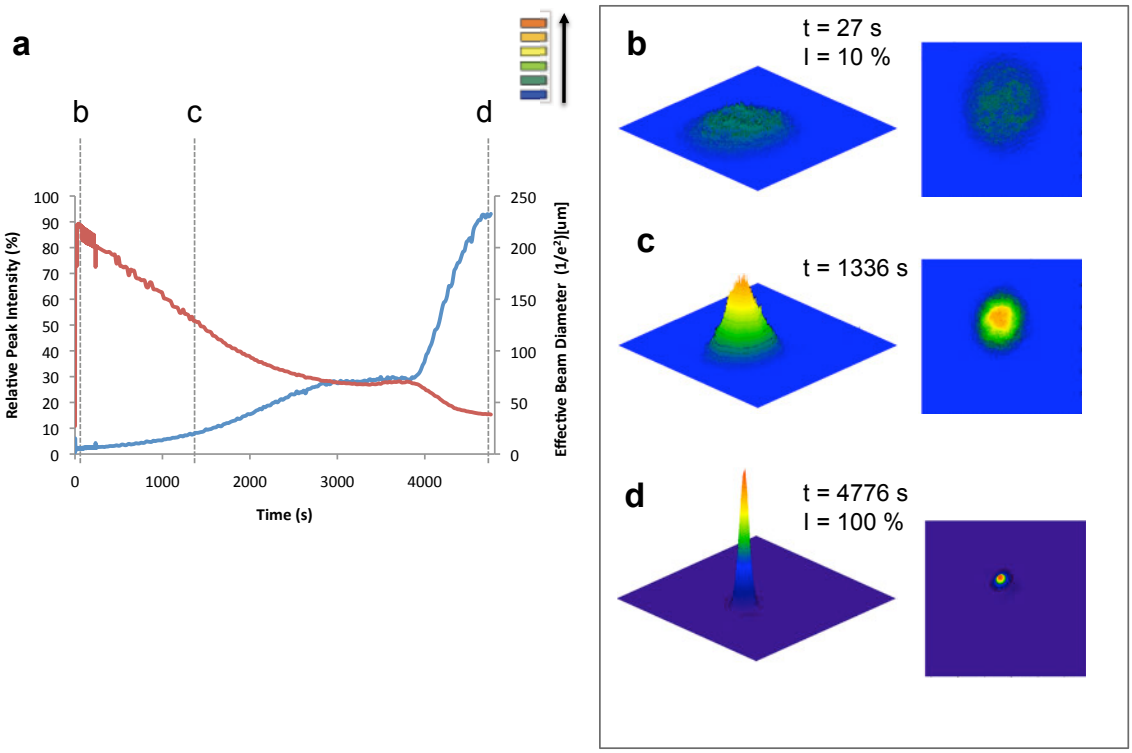

Figure S15 Optical self-trapping with Pluronic® F-127 gel containing 80 μM $Ru(bpy)_3Cl_2$ and 6.0 mM methyl viologen at 159 Wcm^{-2}. The labeled dotted lines in the (a) graph showing temporal evolution of intensity and beam width correspond to (b-d) spatial intensity profiles of the beam.

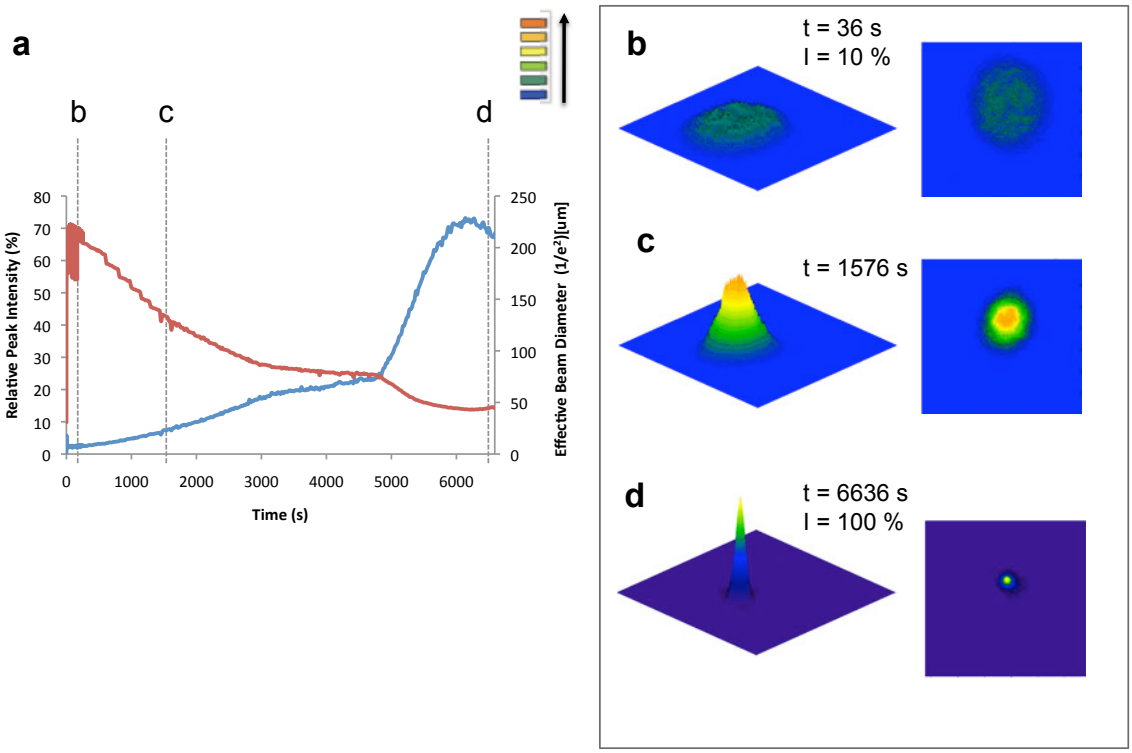

Figure S16 Optical self-trapping with Pluronic® F-127 gel containing 80 μM $Ru(bpy)_3Cl_2$ and 11.9 mM methyl viologen at 159 Wcm^{-2}. The labeled dotted lines in the (a) graph showing temporal evolution of intensity and beam width correspond to (b-d) spatial intensity profiles of the beam.

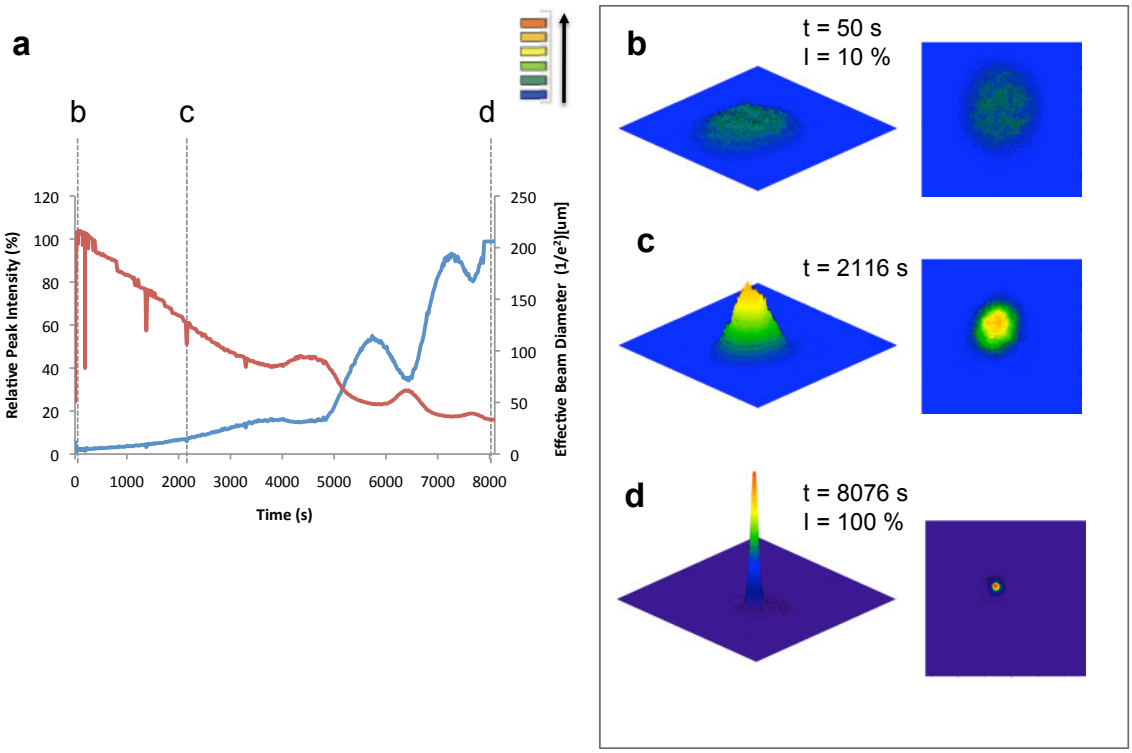

Figure S17 Optical self-trapping with Pluronic® F-127 gel containing 80 μM $Ru(bpy)_3Cl_2$ and 14.8 mM methyl viologen at 159 Wcm^{-2}. The labeled dotted lines in the (a) graph showing temporal evolution of intensity and beam width correspond to (b-d) spatial intensity profiles of the beam.

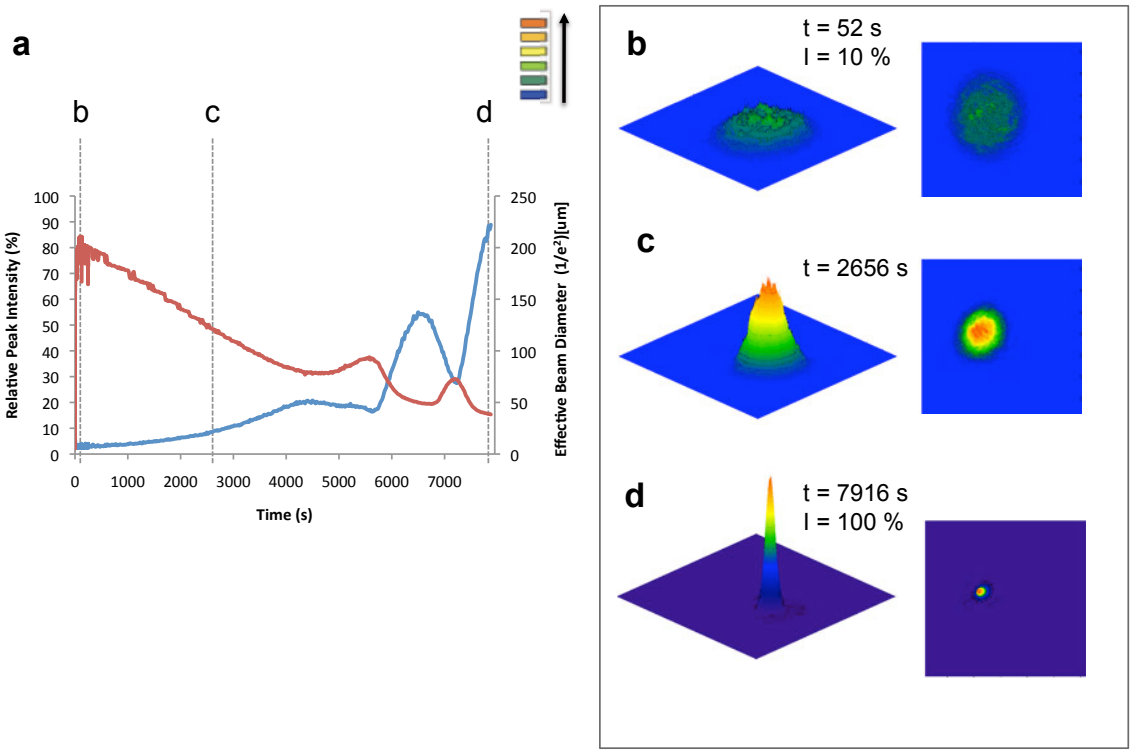

Figure S18 Optical self-trapping with Pluronic® F-127 gel containing 80 μM $Ru(bpy)_3Cl_2$ and 22.9 mM methyl viologen at 159 Wcm^{-2}. The labeled dotted lines in the (a) graph showing temporal evolution of intensity and beam width correspond to (b-d) spatial intensity profiles of the beam.

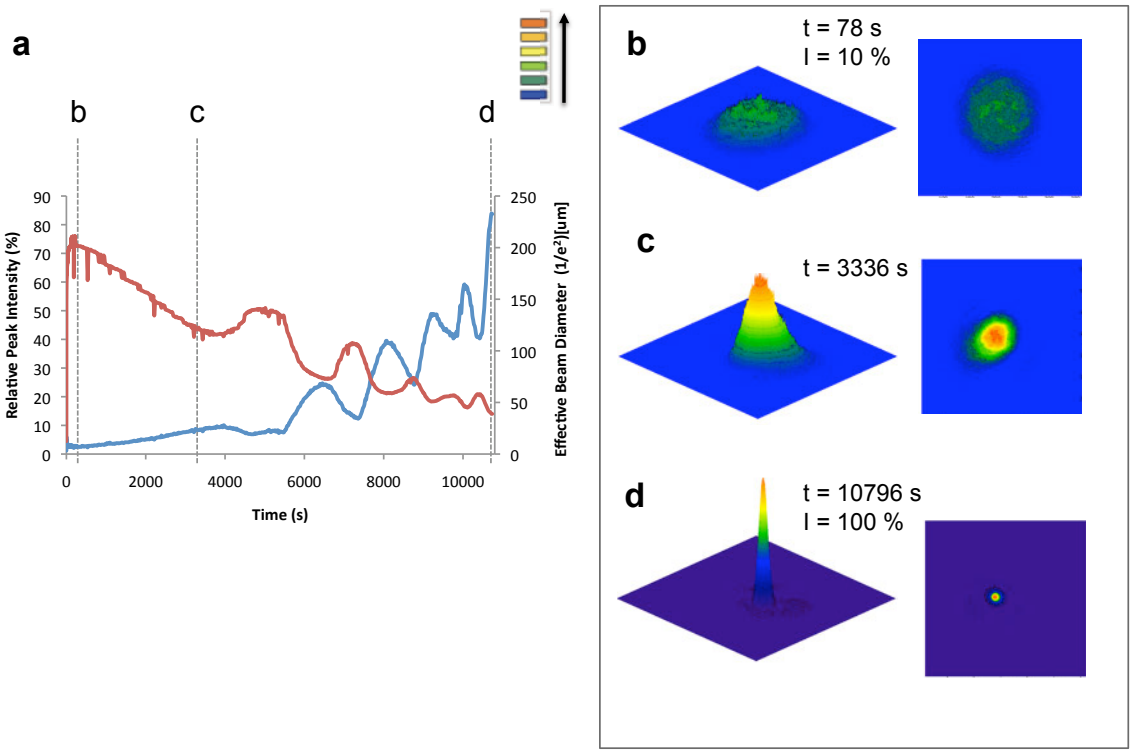

Figure S19 Optical self-trapping with Pluronic® F-127 gel containing 80 μM $Ru(bpy)_3Cl_2$ and 35.7 mM methyl viologen at 159 Wcm^{-2}. The labeled dotted lines in the (a) graph showing temporal evolution of intensity and beam width correspond to (b-d) spatial intensity profiles of the beam.

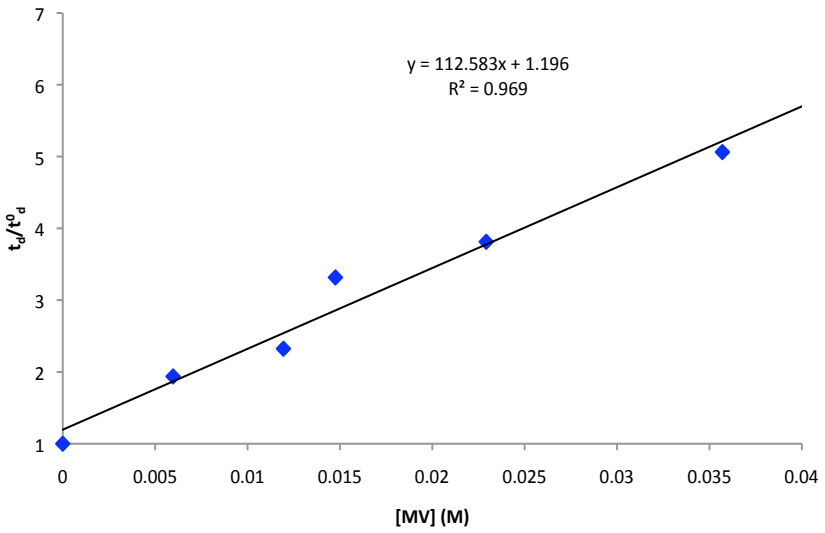

Figure S20 Stern-Volmer plot for self-trapping in Pluronic® gels containing tris(bipyridine)ruthenium(II) chloride and methyl viologen dichloride.

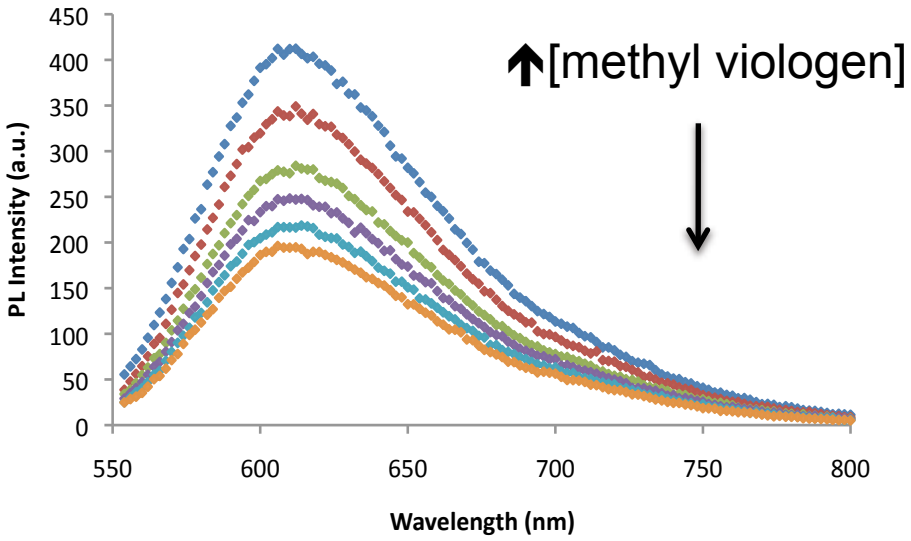

Figure S21 Photoluminescence spectra of $Ru(bpy)_3^{2+}$ in Pluronic® gels as the concentration of methyl viologen increases. Increased concentration of quencher results in decreased photoluminescence.

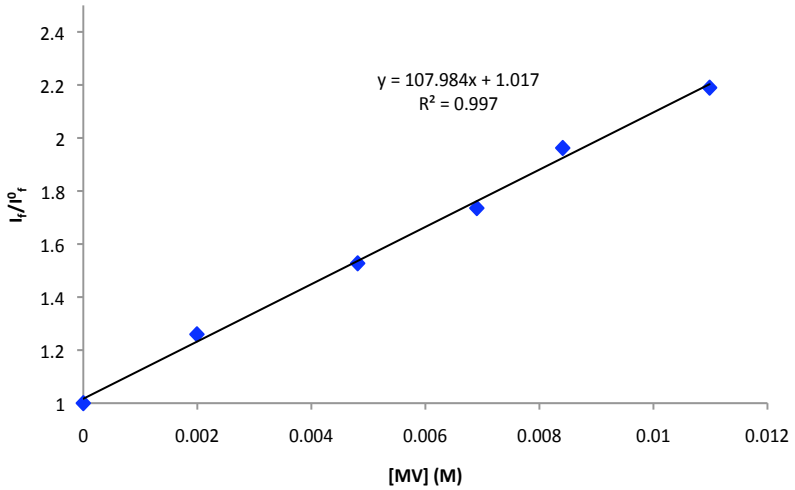

Figure S22 Stern Volmer-plot for photoluminescence in Pluronic® gels containing tris(bipyridine)ruthenium(II) chloride (80 µM) and methyl viologen dichloride (0 mM-12 mM).

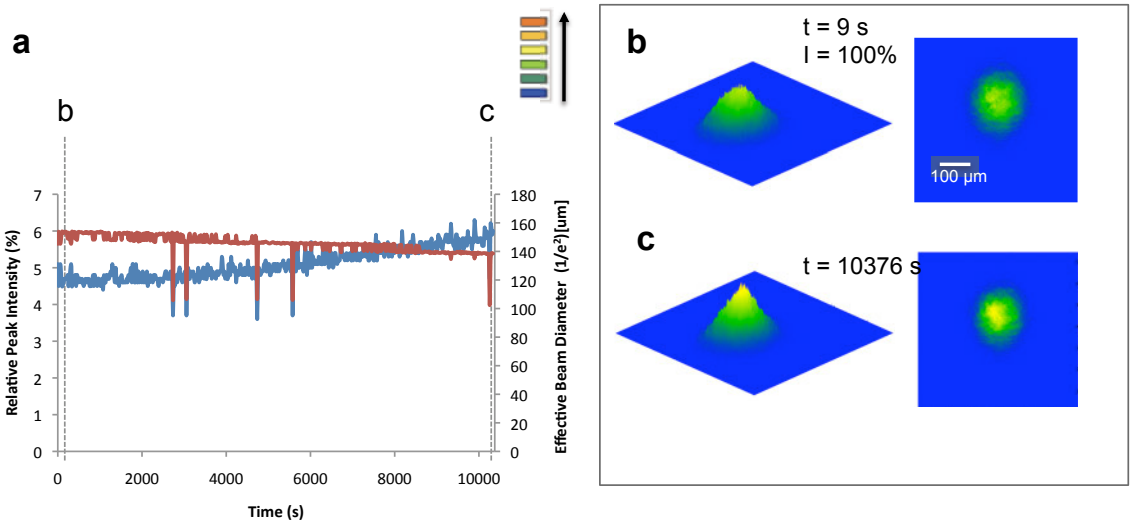

Figure S23 Self-trapping in Pluronic® gels containing tris(bipyridine)ruthenium(II) chloride in the presence of furfuryl alcohol. The labeled dotted lines in the graph showing temporal evolution of beam intensity and diameter correspond to (b-c) spatial intensity profiles of the beam.

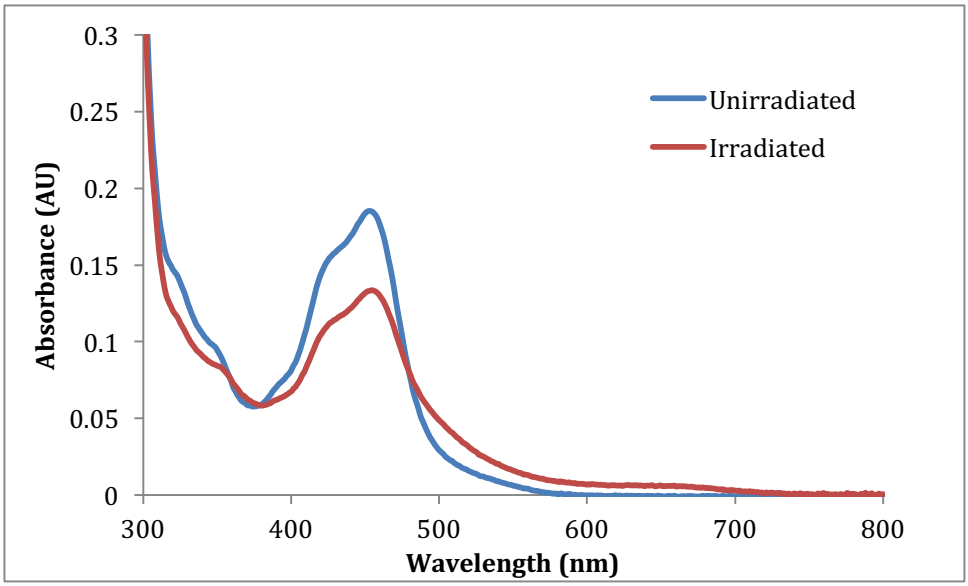

Figure S24 UV-visible absorbance spectrum of $Ru(bpy)_3^{2+}$ in 25% Pluronic® F-127 gel before and after extended irradiation at high intensities.

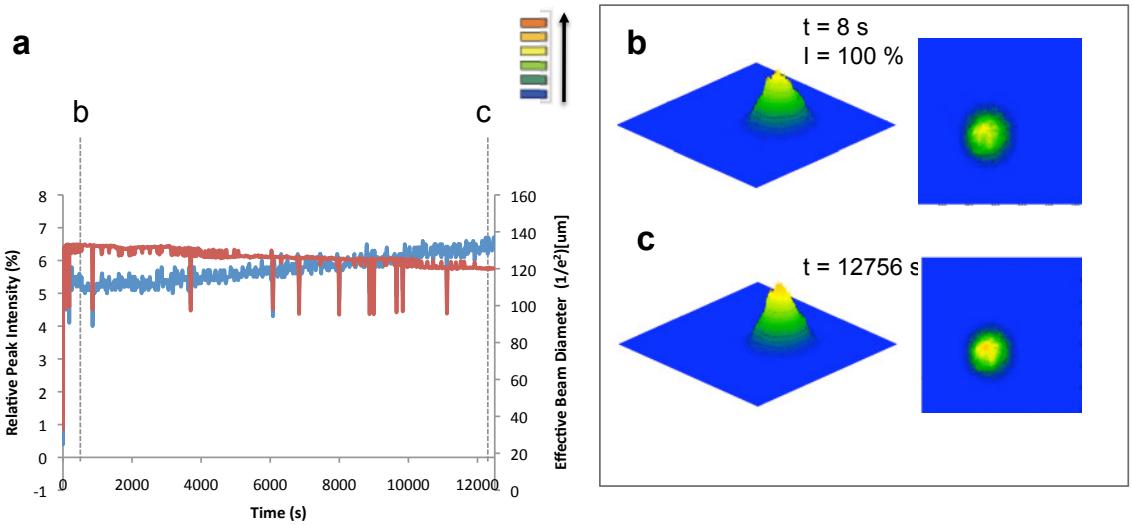

Figure S25 Optical self-trapping with Pluronic® F-127 gel containing 5 mM methyl violet at 159 Wcm^{-2}. The labeled dotted lines in the graph showing temporal evolution of beam intensity and diameter correspond to (b-c) spatial intensity profiles of the beam.

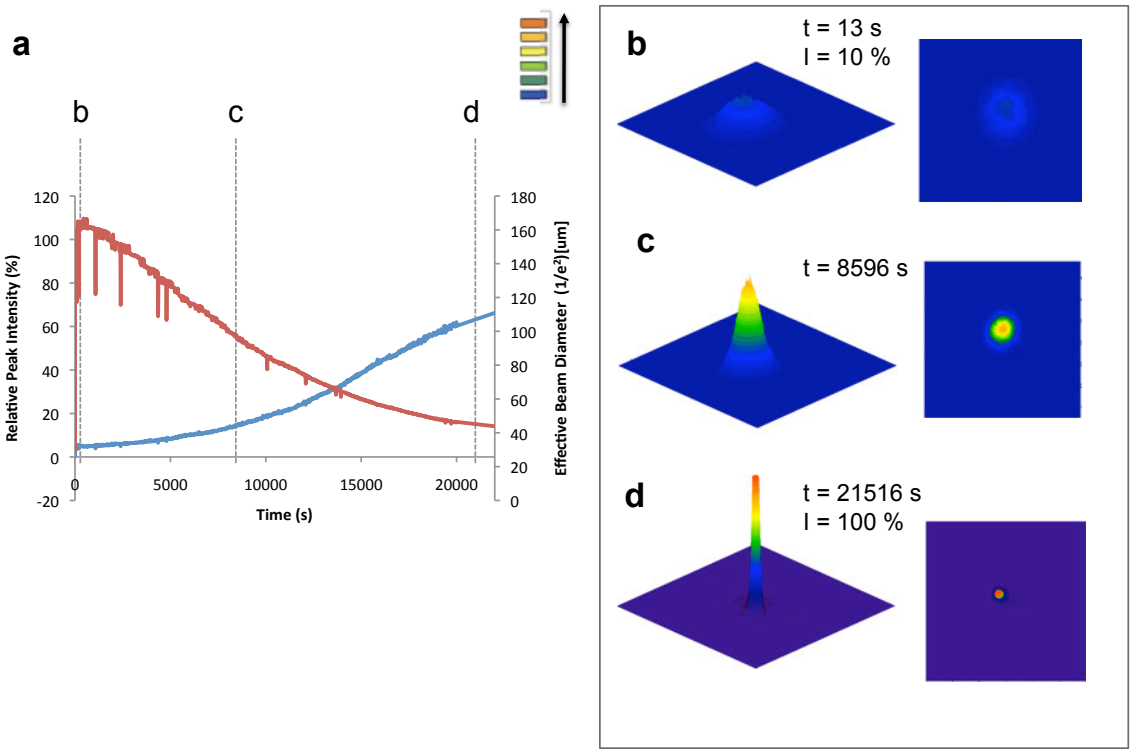

Figure S26 Optical self-trapping with Pluronic® F-127 gel containing 400 µM fluorescein at 159 Wcm^{-2}. The labeled dotted lines in the graph showing temporal evolution of beam intensity and diameter correspond to (b-d) spatial intensity profiles of the beam.

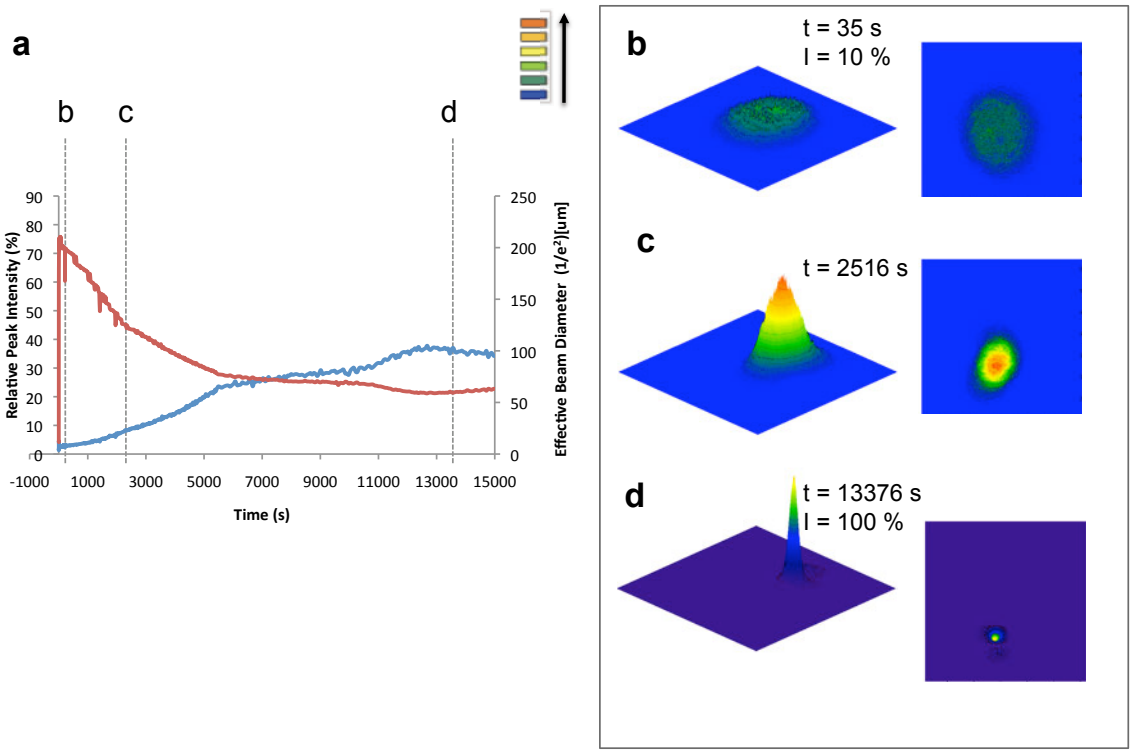

Figure S27 Optical self-trapping with Pluronic® F-127 gel containing 400 µM rhodamine B at 159 Wcm^{-2}. The labeled dotted lines in the graph showing temporal evolution of beam intensity and diameter correspond to (b-c) spatial intensity profiles of the beam.

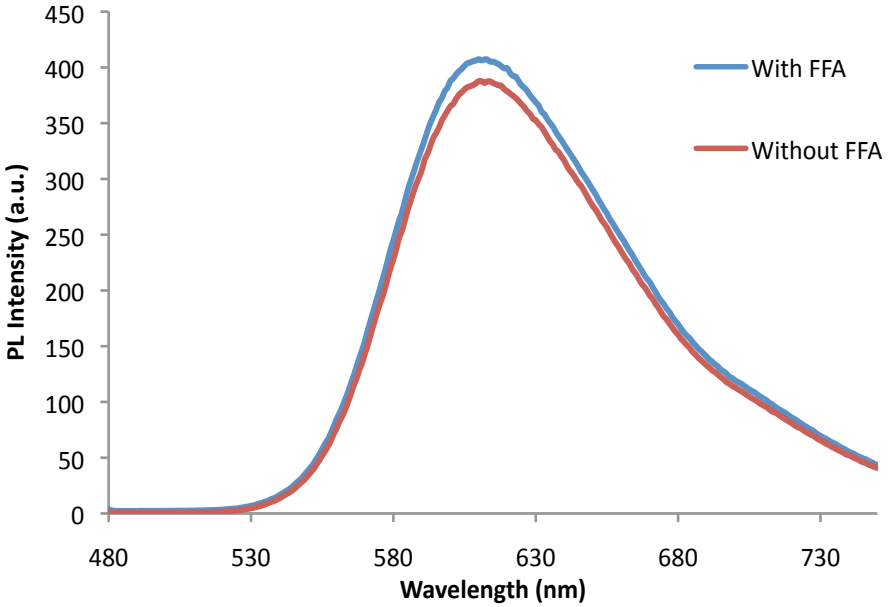

Figure S28 UV-visible emission spectrum of $Ru(bpy)_3^{2+}$ in H_2O with and without furfuryl alcohol (FFA).

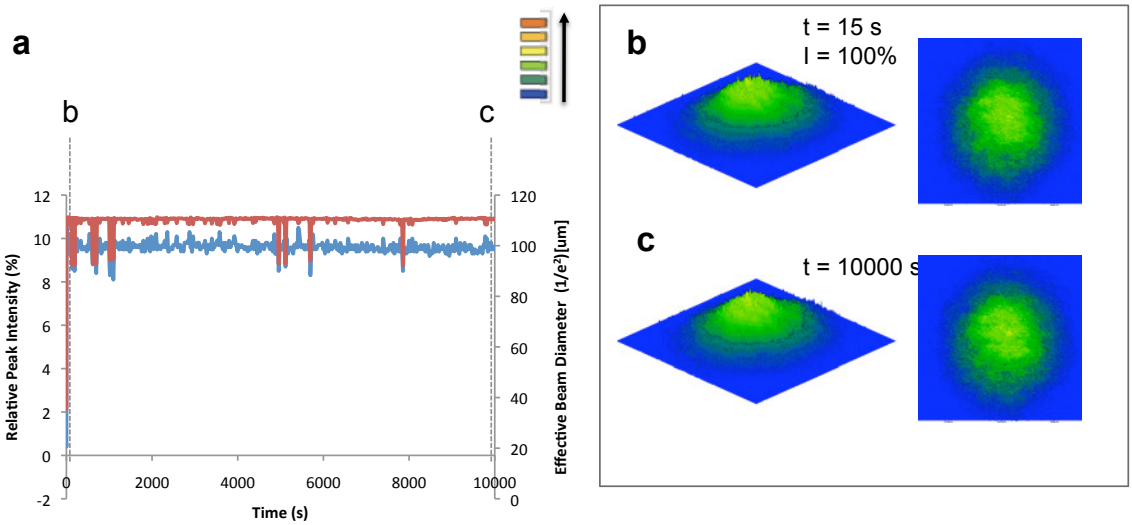

Figure S29 Optical self-trapping in an aqueous solution containing 80 μM $Ru(bpy)_3Cl_2$ at 159 Wcm^{-2}. The labeled dotted lines in the graph showing temporal evolution of beam intensity and diameter correspond to (b-c) spatial intensity profiles of the beam.

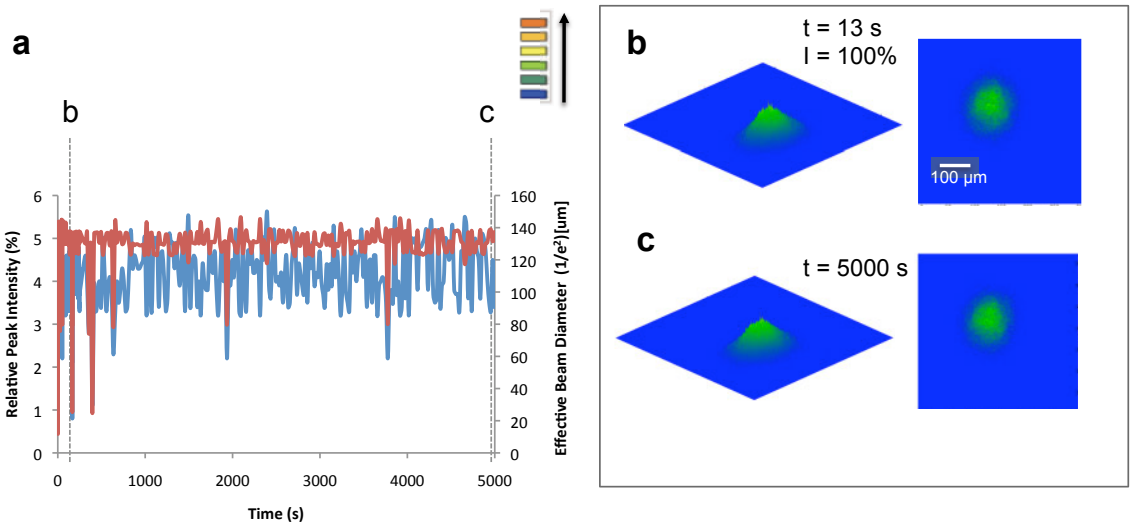

Figure S30 Optical self-trapping within a siloxane gel containing 12 µM $Ru(bpy)_3Cl_2$ at 159 Wcm^{-2}. The labeled dotted lines correspond to the included spatial intensity profiles. The labeled dotted lines in the graph showing temporal evolution of beam intensity and diameter correspond to (b-c) spatial intensity profiles of the beam.

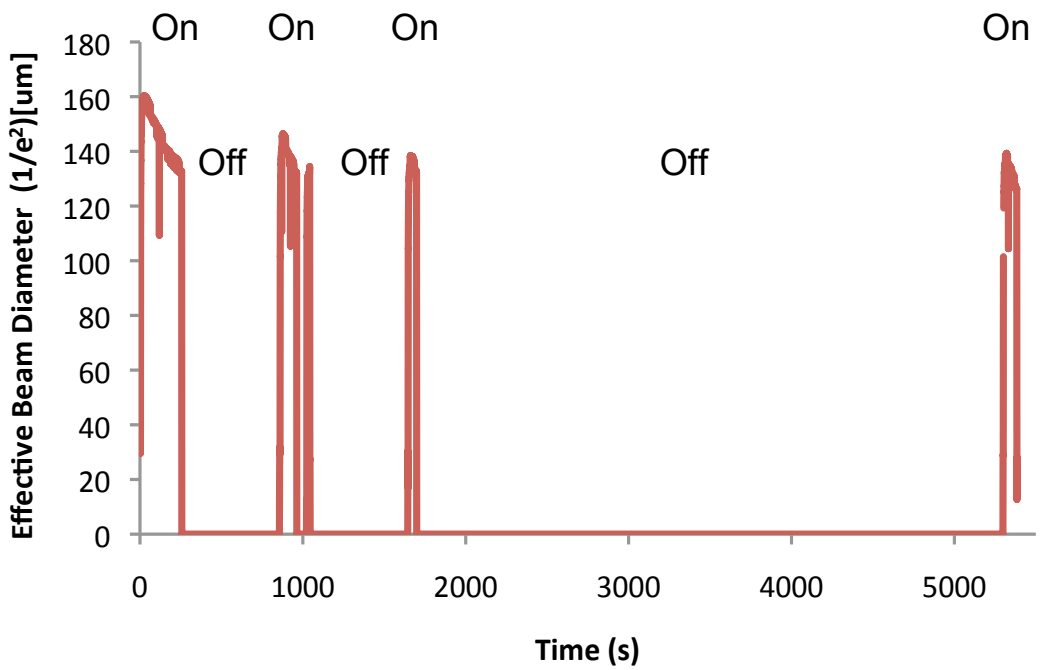

Figure S31 Optical self-trapping of a Pluronic® F-127 gel containing $Ru(bpy)_3^{2+}$ at 159 Wcm^{-2}; the beam was blocked for extended periods of time in order to determine that the system is irreversible. "On" denotes that the beam is incident on the sample and "Off" denotes that the beam has been blocked to allow the sample to relax. The beam profile does not change even when blocked for over an hour, suggesting an irreversible process has occurred.

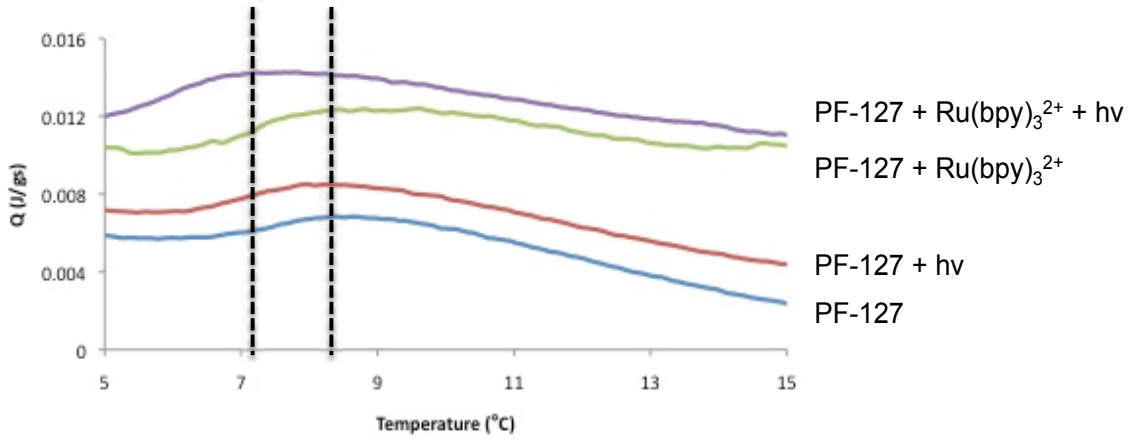

Figure S32 DSC traces for Pluronic® F-127 gels with and without $Ru(bpy)_3^{2+}$. Scans were acquired for both samples prior to and after irradiation.

Section 4. Description of movies

MOVIE_S1
Optical self-trapping due to Iodide oxidation
Temporal evolution and dynamics of the spatial intensity profile of laser beam (532 nm, 8 Wcm^{-2}) at the exit face of a 25% Pluronic® F-127 gel containing 1.3 mM $Ru(bpy)_3Cl_2$ and 0.2 M sodium iodide.

MOVIE_S2
Optical self-trapping due to oxidation of Pluronic® F-127
Temporal evolution and dynamics of the spatial intensity profile of laser beam (532 nm, 159 Wcm^{-2}) at the exit face of a 25% Pluronic F-127 gel doped with 12 μM $Ru(bpy)_3Cl_2$ compared to a 25% Pluronic F-127 gel without $Ru(bpy)_3Cl_2$.

Section 5 - References

(1) Villafranca, A. B.; Saravanamuttu, K. An Experimental Study of the Dynamics and Temporal Evolution of Self-Trapped Laser Beams in a Photopolymerizable Organosiloxane. *J. Phys. Chem. C* **2008**, *112*, 17388–17396.

(2) Villafranca, Ana; Saravanamuttu, K. Spontaneous and Sequential Transitions of a Gaussian Beam into Diffraction Rings, Single Ring and Circular Array of Filaments in a Photopolymer. *Opt. Express* **2011**, *19*, 15560–15573.

(3) Wallace, W. M.; Hoggard, P. E. A Simple Photochemical Synthesis of Some Bis (bipyridyl) Ruthenium (II) Complexes. *Inorg. Chem.* **1979**, *18*, 2934–2935.

(4) De Jong, J. J. D.; Hania, P. R.; Pugžlys, A.; Lucas, L. N.; de Loos, M.; Kellogg, R. M.; Feringa, B. L.; Duppen, K.; van Esch, J. H. Light-Driven Dynamic Pattern Formation. *Angew. Chemie Int. Ed.* **2005**, *44*, 2373–2376.

(5) Delaire, J. a; Nakatani, K. Linear and Nonlinear Optical Properties of Photochromic Molecules and Materials. *Chem. Rev.* **2000**, *100*, 1817–1846.

(6) Zhang, B. Z.; Wang, H. C.; She, W. L. Influence of Molecular Reorientation on Photoisomerization Optical Spatial Solitons. *J. Opt. A Pure Appl. Opt.* **2007**, *9*, 395.

(7) Mandal, B. K.; Kumar, J.; Huang, J.-C.; Tripathy, S. Novel Photo-Crosslinked Nonlinear Optical Polymers. *Die Makromol. Chemie, Rapid Commun.* **1991**, *12*, 63–68.

(8) Morton Z. Hoffman, Fabrizio Bolletta, Luca Moggi, and G. L. H. Rate Constants for the Quenching of Excited States of Metal Complexes in Fluid Solution. *J. Phys. Chem. Ref. Data* **1989**, *18*, 219–543.

(9) DeRosa, M. C.; Crutchley, R. J. Photosensitized Singlet Oxygen and Its Applications. *Coord. Chem. Rev.* **2002**, *233-234*, 351–371.

(10) Haag, W. R.; Hoigne´, J.; Gassman, E.; Braun, A. Singlet Oxygen in Surface Waters — Part I: Furfuryl Alcohol as a Trapping Agent. *Chemosphere*. **1984**, *13,* 631–640.

(11) Kubin, R. F.; Fletcher, A. N. Fluorescence Quantum Yields of Some Rhodamine Dyes. *J. Lumin.* **1983**, *27*, 455–462.

(12) Gandin, E.; Lion, Y.; de Vorst, A. Quantum Yield of Singlet Oxygen Production by Xanthene Derivatives. *Photochem. Photobiol.* **1983**, *37*, 271–278.

(13) Park, H.; Na, K. Conjugation of the Photosensitizer Chlorin e6 to Pluronic F127 for Enhanced Cellular Internalization for Photodynamic Therapy. *Biomaterials* **2013**, *34*, 6992–7000.

(14) Choi, M. M. F.; Xiao, D. Single Standard Calibration for an Optical Oxygen Sensor Based on Luminescence Quenching of a Ruthenium Complex. *Anal. Chim. Acta* **2000**, *403*, 57–65.

(15) Sortino, S.; Petralia, S.; Boscà, F.; Miranda, M. A. Irreversible Photo-Oxidation of Propranolol Triggered by Self-Photogenerated Singlet Molecular Oxygen. *Photochem. Photobiol. Sci.* **2002**, *1*, 136–140.

(16) Ibusuki, S.; Halbesma, G. J.; Randolph, M. A.; Redmond, R. W.; Kochevar, I. E.; Gill, T. J. Photochemically Cross-Linked Collagen Gels as Three-Dimensional Scaffolds for Tissue Engineering. *Tissue Eng.* **2007**, *13*, 1995–2001.

(17) Yousif, E.; Haddad, R. Photodegradation and Photostabilization of Polymers, Especially Polystyrene: Review. *Springerplus* **2013**, *2*, 398.

(18) Rabek, J. F. *Photostabilization of Polymers: Priciples and Application*; Springer Science & Business Media, 2012.